

An Experimental and Computational Investigation of Bone Formation in Mechanically Loaded Trabecular Bone Explants

E. BIRMINGHAM,¹ G. L. NIEBUR,² L. M. MCNAMARA,¹ and P. E. MCHUGH¹

¹Biomechanics Research Centre (BMEC), Biomedical Engineering, College of Engineering and Informatics, National University of Ireland Galway, Galway, Ireland; and ²Bioengineering Graduate Program, University of Notre Dame, Notre Dame, IN 46556, USA

(Received 4 February 2015; accepted 26 June 2015; published online 25 July 2015)

Associate Editor Sean S. Kohles oversaw the review of this article.

Abstract—Understanding how bone marrow multipotent stromal cells (MSCs) contribute to new bone formation and remodeling *in vivo* is of principal importance for informing the development of effective bone tissue engineering strategies *in vitro*. However, the precise *in situ* stimuli that MSCs experience have not been fully established. The shear stress generated within the bone marrow of physiologically loaded samples has never been determined, but could be playing an important role in the generation of sufficient stimulus for MSCs to undergo osteogenic differentiation. In this study fluid structure interaction (FSI) computational models were used in conjunction with a bioreactor which physiologically compresses explanted trabecular bone samples to determine whether MSCs can be directly stimulated by mechanical cues within the bone marrow. Experimentally loaded samples were found to have greater osteogenic activity, as verified by bone histomorphometry, compared to control static samples. FSI models demonstrated a linear relationship between increasing shear stress and decreasing bone volume. The FSI models demonstrated that bone strain, not marrow shear stress, was likely the overall driving mechanical signal for new bone formation during compression. However, the shear stress generated in the models is within the range of values which has been shown previously to generate an osteogenic response in MSCs.

Keywords—Bone marrow multipotent stromal cells, Bone tissue engineering, Bone marrow, Fluid structure interaction, Shear stress, Bioreactor, Marrow.

INTRODUCTION

Bone marrow in the pores of trabecular bone is subjected to mechanical cues during activities of daily

living, mediated by the solid structure surrounding it. Recent studies have demonstrated that the shear stress generated in marrow can be of significant magnitude to stimulate an osteogenic response in the bone marrow cells.^{3,4,13,16,30,42} The magnitude of shear stress required to generate an osteogenic responses in MSCs and pre-osteoblastic cells *in vitro* is commonly reported to range between 0.1 and 1 Pa.^{1,2,11} Other studies have suggested a lower threshold <0.05 Pa^{10,39} and have demonstrated no significant difference in the osteogenic response between osteoblastic cells exposed to either 0.06 or 0.6 Pa.³³ However, the response of marrow cells to this shear stress generated during physiological loading has yet to be determined.

Bone is understood to adapt its structure in response to changes in mechanical forces. This is believed to be mediated by a mechanostat approach¹⁹ where bone resorption due to disuse is initiated at a compressive strain level of less than 1000 $\mu\epsilon$,¹⁹ and vigorous exercise generates compressive strains up to 3000 $\mu\epsilon$ which stimulates new bone formation.^{8,18} However, compressive strains of greater than 3500 $\mu\epsilon$ can lead to damage, resorption and fracture of bone.^{9,32}

Osteocytes are the primary mechanosensors in bone remodeling.^{6,23,40} They are found embedded throughout the bone matrix with numerous projections extending outwards into the matrix. It is thought that osteocytes act as a network of strain gages monitoring the mechanical environment directly and recruiting other cells to alter the bone mass as required.⁴³ Osteocytes have been shown to direct the differentiation of MSCs in a simplified bone marrow stem cell niche.⁵ However, due to the presence of shear stress which is generated within bone marrow during physiological loading there is a potential role for the direct

Address correspondence to E. Birmingham, Biomechanics Research Centre (BMEC), Biomedical Engineering, College of Engineering and Informatics, National University of Ireland Galway, Galway, Ireland. Electronic mail: evelyn.birmingham@gmail.com

stimulation of MSC cells in the marrow to undergo osteogenic differentiation.^{12,21,22} If this were to be the case it could augment the osteocyte mediated strain response of bone.²⁰

In vitro studies of trabecular bone explants have previously been used to examine bone formation in response to compression of the bone matrix.^{14,15,17,24,29,44} Greater bone growth attributed to bone strain was found in samples exposed to the mechanical loading compared to control static samples,^{14,29} reproducing the *in vivo* effects of mechanical strain on bone growth.

In the present work ovine trabecular bone explants were exposed to compression in a custom built bioreactor in a similar manner to the previous studies.^{14,15,17,24,29,44} The objective was to examine whether the shear stress generated in trabecular bone marrow due to physiological compression of bone was of a sufficient magnitude to generate an anabolic response in the bone. μ -CT scans of experimental bone explants were used to generate the meshes for computational analysis. A fluid structure interaction (FSI) computational approach developed previously³ was applied to the specimen specific geometries to determine the strain in the bone and the corresponding marrow shear stress in the experimental samples. Mechanically loaded samples were compared to control samples (which experienced no loading) using fluorochrome-based bone histomorphometric methods that determine the level of bone growth within the samples. These techniques allow for the determination of the relative roles of bone strain and shear stress in formation of new trabecular bone. In this way the study generates important insights into the mechanical cues for generating an anabolic response in bone.

METHODS

Harvest of Bone Explants

Bone explants were harvested in an approach similar to previous studies.^{15,29} Briefly, ovine vertebrae (C1–C2) were obtained from the slaughterhouse fresh from slaughter. Working in sterile conditions, skin, muscle and flesh were removed, and the vertebrae were dissected apart. The superior endplates were cut off to reveal the trabecular bone beneath. Using a diamond coring drill (Eternal Tools, Worcestershire, UK) 8 mm diameter trabecular bone explants 15–20 mm long were prepared from the C2 vertebrae. All cutting was performed under constant irrigation using ice cold PBS and 5% antibiotic antimycotic (AB-AM, Sigma Aldrich). Bone explants were stored in cold PBS with AB-AM until parallel ends were cut using a low speed

diamond saw (Buehler, Lake Bluff, IL) to approximately 10 mm lengths. Bone explants were then placed in media overnight, containing DMEM, 10% FBS, 2% AB-AM, 20 mM β -glycerol phosphate and 50 μ M L-Ascorbic acid 2-phosphate sesquimagnesium salt hydrate (AA2P, Sigma Aldrich). Steps were taken to ensure that this preparation time was not longer than 3 h post slaughter to limit cell death and damage.

The bone explants were then divided into control and loading groups. The Control samples ($n = 4$) were kept in media in 6 well plates. Media was changed every other day. On day 7 calcein blue (Sigma Aldrich) at a concentration of 50 μ g/ml was added to the media, this was replaced with fresh media the following day. On day 14 alizarin red was added to the media at the same concentration of 50 μ g/ml, this media was again replaced on day 15. After 21 days of culture, bone cores were washed with PBS and fixed in 10% formalin for 5 days. These control samples were not exposed to any loading.

Compression Bioreactor

Compression was applied to the bone explants in the loaded group ($n = 4$) through the use of an adapted Enduratec bioreactor (Bose Limited, Gillingham, UK). This was customized in-house to provide physiological loading to trabecular bone cores. This device was similar to the previously reported Zetos devices^{15,24} (Fig. 1). A chamber which provided a compressive loading regime to the bone explants was attached to the actuator. The bone explant was held between a fixed bar which was attached to a load cell in the top of the chamber and the moving bar controlled by the actuator (Fig. 2). Media was circulated continuously through the system by a peristaltic pump (Cole Palmer, Dublin, Ireland). Platinum-cured silicone tubing (Cole Palmer) was used to allow for oxygen and carbon dioxide exchange.

A cyclic (1 Hz sine wave) compression applying 2000 μ ϵ compressive nominal strain to the bone explants for 10 min was applied for 15 days in a total of 21 days culture. This loading condition was representative of strains generated in mouse trabecular bone during caudal vertebral axial compression⁴⁵ and this strain has been shown to correspond to trabecular bone generation.⁴¹ Additionally, this level of strain has generated significant trabecular bone growth in a previous study on *ex vivo* bone growth in trabecular explants.¹⁴

On day 7 calcein blue (50 μ g/ml) was added to the media. This media was then filtered in order to re-sterilize it. This was replaced with fresh media which was allowed to circulate through the system for 8 h the following day, before being replaced with fresh media.

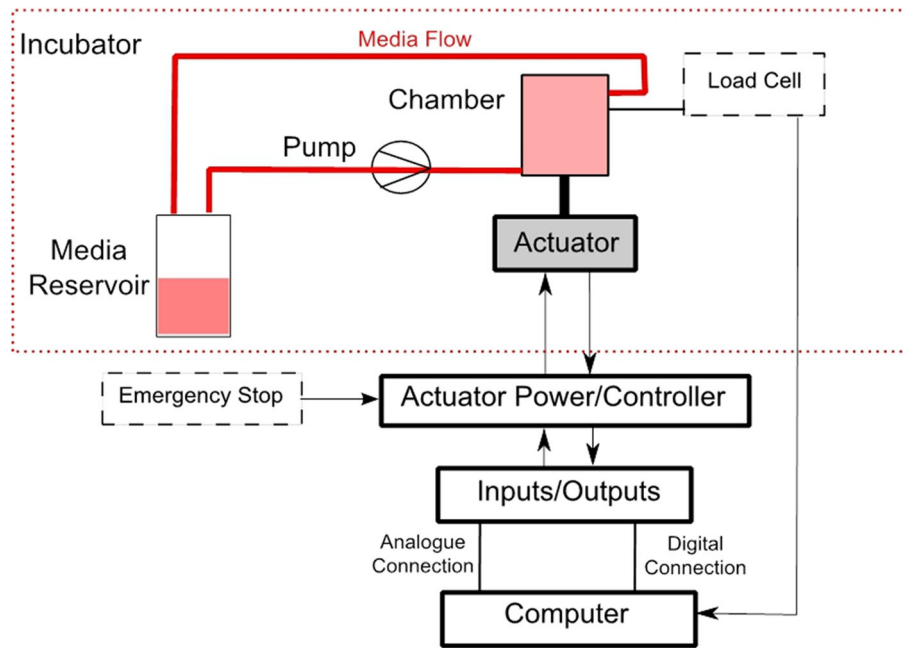


FIGURE 1. Flow schematic of the bioreactor structure. Media was pumped through the chamber and returns to the reservoir. Displacement was inputted to control the displacement of the actuator; a load cell relays the resulting force. The pump, media reservoir, tubing, chamber, load cell and actuator were all kept within the incubator.

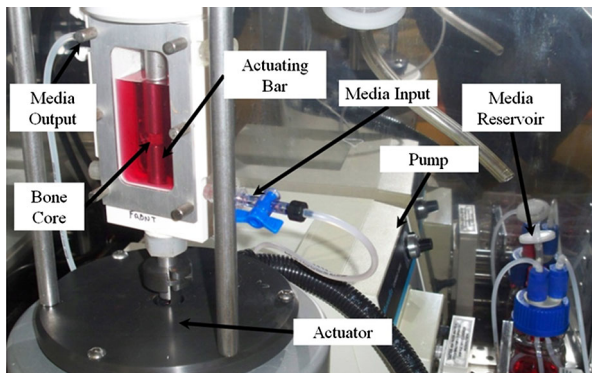


FIGURE 2. Photo of the bioreactor with actuator, chamber and pump in the incubator.

On day 14 alizarin red was added to the media at the same concentration of $50 \mu\text{g/ml}$ and filtered to re-sterilize. This media was again replaced on day 15 with fresh media which was allowed to circulate for 8 h before being replaced with more fresh media. After 21 days of culture, bone cores were washed with PBS and fixed in 10% formalin for 5 days and scanned using a Scanco μCT40 MicroCT Scanner at a resolution of $16 \mu\text{m}$.

Histomorphometry Analysis

After fixation in formalin, both the control static explants and the explants exposed to loading were dehydrated in increasing concentrations of ethanol.³¹

Explants were then infiltrated overnight and embedded in polymethylmethacrylate (Osteo-Bed Bone Embedding Kit, Sigma Aldrich). Thin sections were cut using the low speed diamond saw to approximately $200 \mu\text{m}$ thicknesses and polished with decreasing grit size silicon carbide paper until the required thickness ($60\text{--}100 \mu\text{m}$) and surface finish was obtained. Sections were then mounted on microscope slides using DPX.

Images were obtained using an Olympus Inverted Fluorescent Microscope IX51 microscope with DAPI-5060c and U-MWG2 filters to visualize the Calcein Blue and Alizarin Red respectively. Four sections in total were taken from each bone core with five images taken from each section at the magnification of $\times 10$, giving a total of twenty images per sample. From each section bone labeling was quantified using ImageJ (NIH). The mineralising surface (MS) was calculated in each image as the length of any double label plus half the length of any single label divided by the overall bone surface (BS). MS is dimensionless and expressed here in percent. The mineral apposition rate (MAR) was estimated by the mean distance between the double labels divided by the time period of 7 days (time between the two labels), and is expressed here in units of $[\mu\text{m/day}]$. The bone formation rate (BFR) was derived using the formula: $\text{BFR} = \text{MAR} \times \text{MS}$, also expressed here in units of $[\mu\text{m/day}]$. The nomenclature assigned to the histomorphometric indices complies with the standards outlined by ASBMR Histomorphometry Nomenclature Committee.³⁴

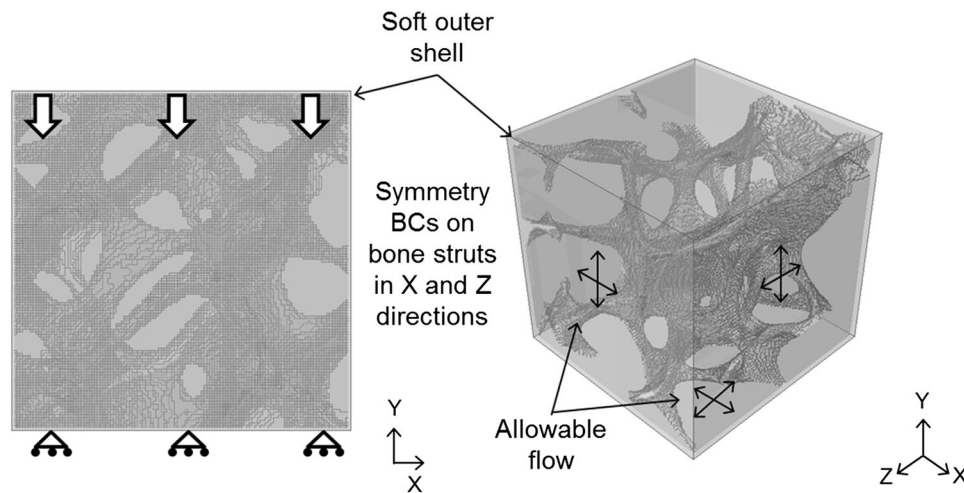


FIGURE 3. Boundary conditions applied to the realistic geometries, following the approach in Birmingham *et al.*³ Symmetry deformation constraints were applied to the boundaries of the fluid domain through the use of a soft outer shell; this was used to explicitly constrain the unit cell boundary both fluid and solid to remain cuboidal during deformation, by coupling the displacements, in the direction normal to the respective faces, of all nodes to a master node on the inside surface. Casing layer of elements and marrow are transparent for clarity in images.

FSI Modeling

Finite element (FE) voxel meshes for models of the four loaded samples were generated using Mimics (Materialise, Belgium), and loading simulations performed using Abaqus (v 6.12 DS SIMULIA, RI, USA). The marrow part was created as the inverse of the bone region. Bone and marrow cubes of 1.6 mm^3 were analyzed within the center of each sample. C3D8R elements were used for the solid bone domain with bone mesh sizes (including the outer casing layer of elements) of $1.35\text{E}5$, $2.17\text{E}5$, $2.97\text{E}5$ and $2.46\text{E}5$ for the 4 analyzes. FC3D8 elements were used for the fluid domain with marrow mesh sizes of $7.49\text{E}5$, $8.02\text{E}5$, $8.16\text{E}5$ and $8.35\text{E}5$ for the 4 analyzes. Element size was fixed at the voxel size of $16 \mu\text{m}^3$. This gives BV/TV values for the four analyzes of 10.83, 19.62, 28.73 and 22.11%.

Solid (bone) and fluid (marrow) analyzes were fully coupled using the Abaqus co-simulation engine (Gauss–Seidel coupling algorithm), allowing for a two-way coupled FSI. The equations for the solid and fluid models were solved separately, and loads and boundary conditions were exchanged at the interface region. Fluid flow was modeled in an Eulerian domain employing the Arbitrary Lagrangian–Eulerian (ALE) method which is used when the boundaries of the Eulerian domain are moving due to FSI.³⁵ This ALE formulation allows for mesh deformation of the fluid domain.

In these models a soft solid outer case was generated to surround the solid and fluid domains (Fig. 3). This was required in order to implement the required

boundary conditions due to restrictions in coupling nodes between the fluid and solid meshes within Abaqus. A prescribed displacement resulting in an overall compressive strain of $2000 \mu\epsilon$, matching experimental conditions, was applied to a master node on the top surface and all other nodes on the inside/bottom surface of the cap were constrained to move together with the master node in the superior-inferior (Y) direction, using an equation constraint. The equation constraint function in Abaqus ensures all sides remain orthogonal during loading. No constraint was applied to these nodes in the transverse plane (X and Z directions). These boundary conditions, combined with the fact that the cap was of negligible stiffness relative to the bone, ensure that the marrow and bone domains move as one on this boundary without constraining lateral motion of the bone struts on the top surface. Symmetry boundary constraints were applied to the lateral surfaces, again using an equation constraint. These couple the displacements of all nodes on the given strut faces to a master node, for displacement components in the direction normal to the respective face for both struts and the fluid domain. This ensured the sides of the solid bone and marrow domain remain orthogonal during loading, but could displace to allow Poisson expansion of the overall structure. This approach ensured that the fluid domain sides remain orthogonal during loading (matching the solid deformation conditions). Flow was modelled as symmetric in the X and Z directions and on the bottom surface by preventing velocity normal to the respective boundaries. These boundary conditions were arrived at

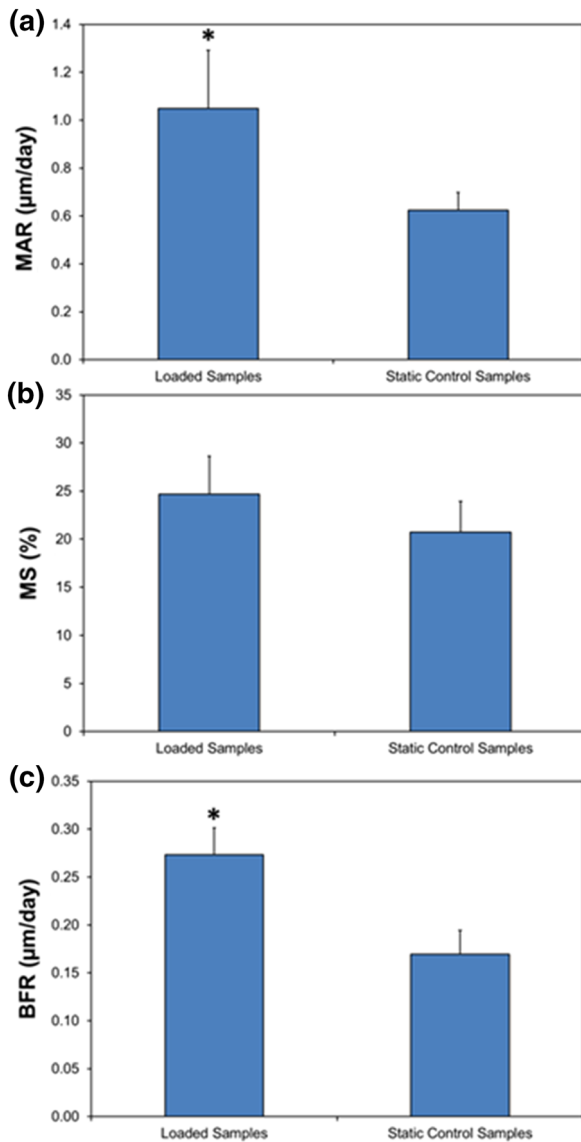


FIGURE 4. (a) Mineral Apposition Rate (MAR) (b) Mineralising Surface (MS) and (c) Bone Formation Rate (BFR) for the loaded and the control static bone explants where asterisk indicates significance between the average values for the loaded group compared to the control static group. $p < 0.05$ as calculated using a paired t test.

following a systematic study of the effects of boundary conditions assumptions described in greater detail in Birmingham *et al.*³

The solid bone deformation was simulated using dynamic implicit analyzes within Abaqus/Standard. An infinitesimal deformation kinematic framework was assumed for the simulations, which is the default kinematic setting for dynamic implicit in Abaqus. This restriction to small strain kinematics was reasonable given the relatively small magnitudes of bone strains considered in these simulations, e.g. 2000 $\mu\epsilon$ equates to only 0.2% compressive strain. Although bending of

some trabeculae during loading may lead to higher local strains.

Bone was modelled as linearly elastic with $E = 15$ GPa and $\nu = 0.3$.²⁶ The soft outer case was also linear elastic with $E = 15$ MPa³ and $\nu = 0.3$. A density of 2 g/cm³ was applied to both. Bone marrow was modelled as a Newtonian fluid with a viscosity of 0.4 Pa.s and a density of 0.9 g/cm³.³⁷ Loading conditions were applied to represent the experimental conditions of a cyclic (1 Hz) compression applying 2000 $\mu\epsilon$ nominal strain to the bone matrix. Shear stress in the marrow was calculated using the reported shear rate based on the second invariant of the rate of deformation tensor and multiplying this by the viscosity.³

Statistical Analysis

A Mann–Whitney Test was used to compare MAR, MS and BFR between the control static samples and the samples exposed to compressive loading. The non-parametric analysis was selected due to the relatively low samples size. Regression analyzes were performed to assess the relationship between shear stress and bone strain/marrow stress as calculated in the computational models. All analyzes were performed with Minitab. For all comparisons, the level of significance was $p \leq 0.05$.

RESULTS

Trabecular Bone Histomorphometry

Analysis of the trabecular sections showed that there was a greater mineral apposition rate for bone explants exposed to compressive loading compared to the explants cultured in control static conditions (MAR $p = 0.0304$, Fig. 4a). There was no significant difference between the two groups for mineralising surface (MS, $p = 0.1939$, Fig. 4b). However, the bone formation rate was greater in the loaded groups compared to the control static group (BFR, $p = 0.0304$, Fig. 4c). Representative images of calcein, alizarin red and double labels are presented in Fig. 5. For clarity, alizarin is red in color with calcein pseudo-colored in green.

FSI Modelling of Trabecular Bone

Bone Strain

The distribution of maximum principal strain is demonstrated for each loaded trabecular bone explant in Fig. 6, where L1, L2, L3 and L4 represent each of the loaded samples. The majority of bone in

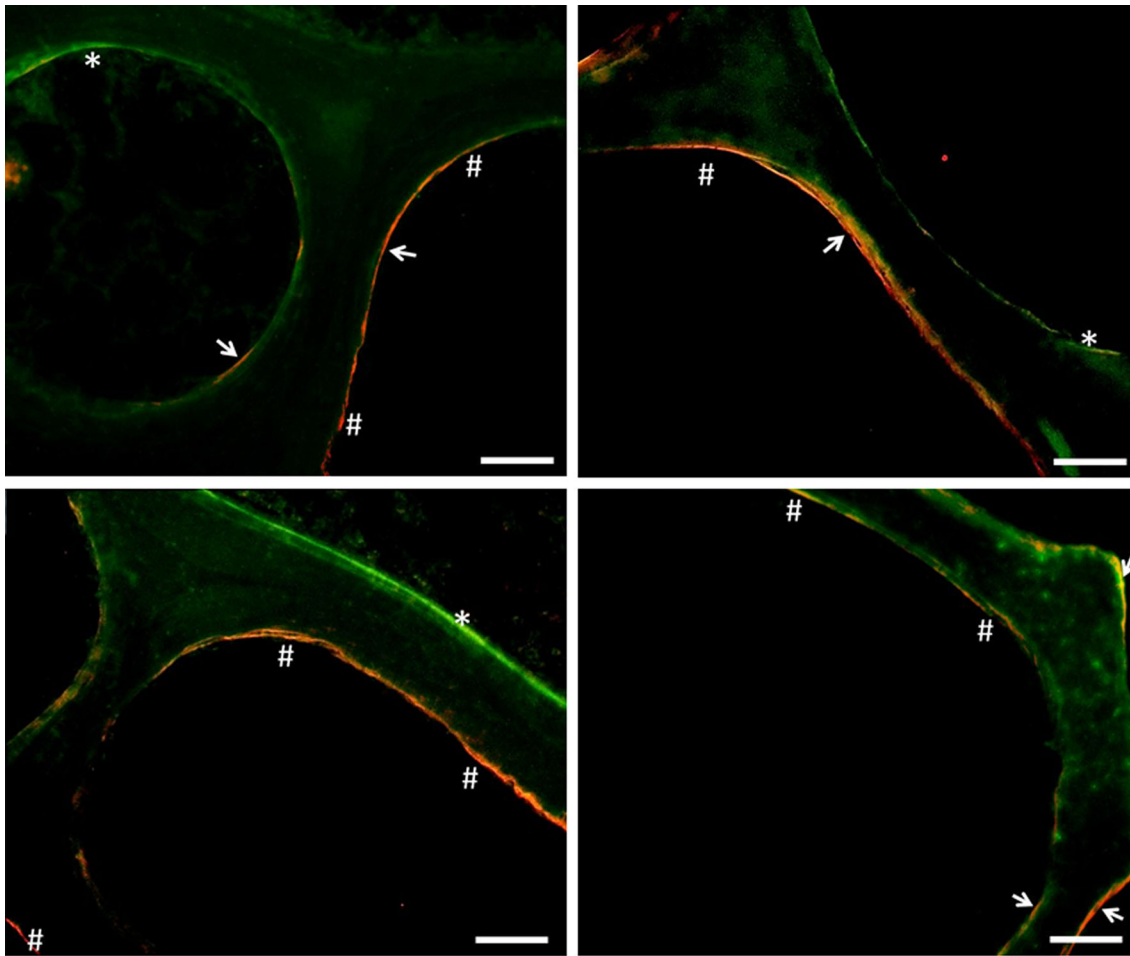


FIGURE 5. Representative images of calcein and alizarin labels. Alizarin (red) labels are indicated with #, calcein (green) labels are indicated with asterisk and double labels are indicated with arrows. All scale bars are 100 μm .

each loaded sample was experiencing compressive strain of less than 1000 $\mu\epsilon$ (88–98%, Table 1). Average values of compressive strains in each sample, ranged from 363 to 635 $\mu\epsilon$. The percentage of bone experiencing compressive strain within the reported stimulatory range (1000–3000 $\mu\epsilon$) for each sample is displayed in Table 1. In addition to strain throughout the bone a particular focus was applied to the strain on the bone surface with elements at the bone/marrow interface analyzed in isolation.

The percentage of bone surface experiencing compressive strain within the reported stimulatory range (1000–3000 $\mu\epsilon$) is displayed in Fig. 7b for each sample. By calculating the strain in the surface elements alone, the amount of elements experiencing less than 1000 $\mu\epsilon$ compressive strain decreased to 83–96%. Additionally the average value of compressive strain across the bone surface increased to 419–677 $\mu\epsilon$ and the percentage of bone experiencing between 1000 and 3000 $\mu\epsilon$ compressive strain was greater at the surface than within the total bone (Table 2).

Shear Stress in Marrow

The distribution of shear stress within the marrow is shown for each trabecular bone explant in Fig. 8. In the mechanically loaded trabecular explants the average shear stress within the marrow was found to range from 0.018 to 0.020 Pa with less than 1% of the marrow in each sample (0.58, 0.22, 0.11 and 0.04%) experiencing greater than 0.1 Pa. The percentage of total marrow experiencing shear stress within the range of 0.01 and 0.1 Pa is displayed in Fig. 9a and summarized in Table 3. When the surface elements alone were examined, the percentage of marrow experiencing stress greater than 0.1 Pa increased in all samples (6.22, 1.57, 1.36 and 0.23%, Fig. 9b and Table 4).

Correlation Between Mechanical Loading and Bone Growth

It was of significant interest to explore potential correlations between the primary variables in the computational modelling and the experiments. No

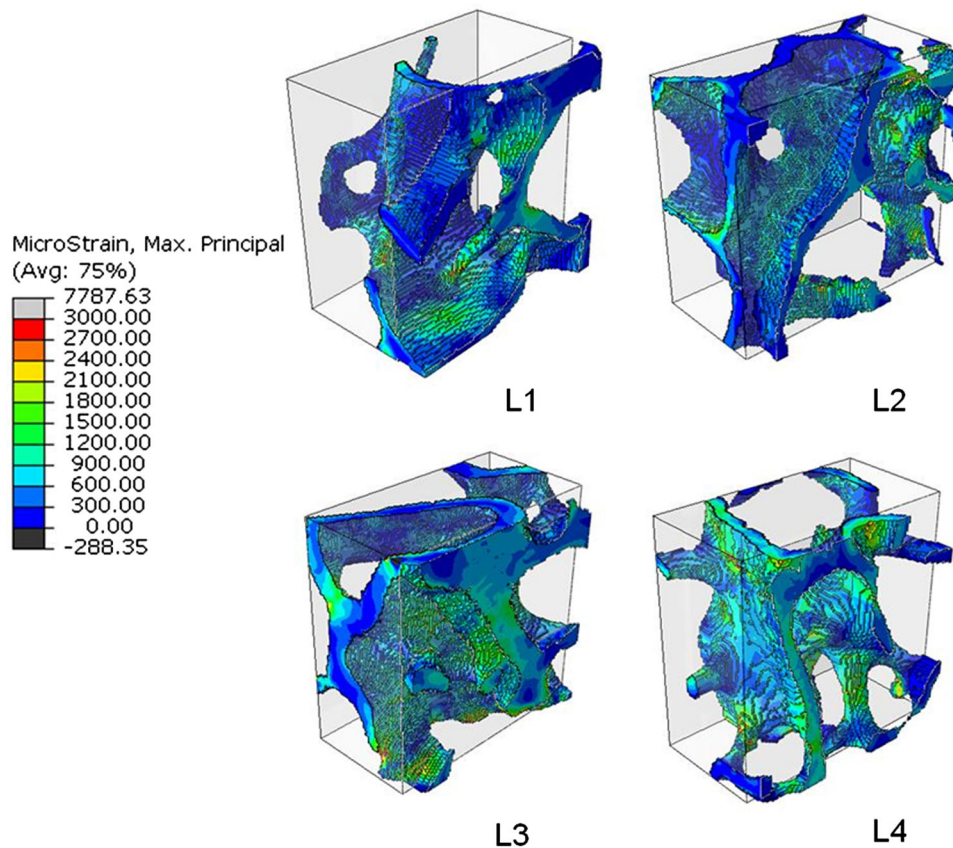


FIGURE 6. Max principal strain in the solid bone of each sample. Samples are sectioned, with the outer case of elements removed and the marrow colored in gray for clarity.

significant correlation was found between specific levels of bone strain or shear stress within each loaded sample and the amount of formed bone, as calculated using MAR, MS and BFR. Figures 10a and 10b demonstrate the lack of correlation between the surface bone strain or surface marrow shear stress calculated from the models and the BFR calculated from the explanted trabecular bone samples exposed to loading. For the simulations, the average shear stress within the marrow was found to be lower in models with higher BV/TV as shown in Fig. 10. This BV/TV was determined post-experiment using the μ -CT scans. A significant correlation was found between average shear stress within the total marrow and the BV/TV. This, however, was not the case for the average surface shear stress. No significant correlation was found between the average strain within the bone ($p = 0.418$) or at the surface ($p = 0.425$) and BV/TV.

DISCUSSION

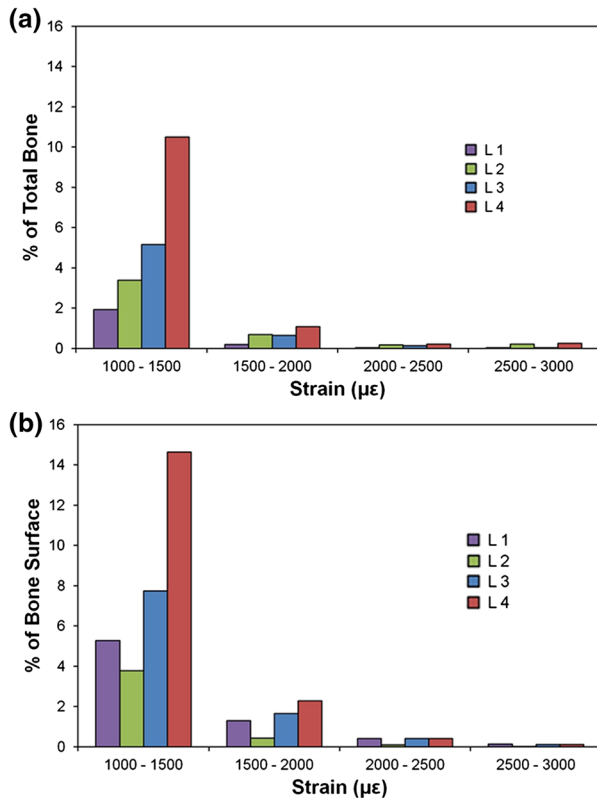
In this study the effect of compressive loading on bone formation in trabecular bone explants was determined through the use of a custom built biore-

actor coupled with computational modelling of the bone and marrow. Bone explants exposed to compressive loading were found to have a significantly higher MAR and BFR compared to the control static explants, demonstrating the anabolic effect of compressive loading in the bone explant model. Computational results show that average shear stress within the marrow ranged from 0.018 to 0.030 Pa, while the average strain experienced in each sample ranged from 363 to 635 $\mu\epsilon$. Bone strain and marrow shear stress were highest in the regions at the bone/marrow surface, and the averages of both shear stress and strain increased when the surfaces alone were examined (0.032 to 0.050 Pa and 419 to 677 $\mu\epsilon$).

Both the control static samples and compressively loaded samples were found to be actively producing new matrix, with mineralising surfaces visible in both cases and with both single and double labels visible. However, the MAR and the BFR were significantly greater in the compressively loaded samples compared to the control static samples. This is in agreement with similar studies that found that the *in vivo* anabolic effects of mechanical strain are reproduced in a trabecular bone explant model.^{14,29} However, to the author's

TABLE 1. The percentage of total bone experiencing strain within different ranges and the average max principal strain within each sample.

Value of max principal strain ($\mu\epsilon$)		Loaded samples			
		L1	L2	L3	L4
% of bone	< 1000	98	96	94	88
	1000–3000	2.2	4.4	6.0	12
	> 3000	0.00	0.03	0.03	0.02
Average max principal strain ($\mu\epsilon$)		363	406	494	635

**FIGURE 7.** Distributions of max principal strain within the bone of each compressively loaded trabecular bone explants for the (a) total bone and (b) at the bone surface.

knowledge, this was the first time the *ex vivo* effects of bone strain have also been examined using a combined computational and experimental approach.

Some limitations of the study include the relatively small sample size and short experiment duration. It would be of significant interest to repeat this study for a longer duration to see if the effects are maintained over time. However, it is not known if this is possible with the explant model as similar models have only been studied up to 3 weeks¹⁴ and 4 weeks.²⁹ Explant models have advantages in that samples can be obtained and maintained relatively easily and cheaply compared to animal models. Additionally, for examining the causes of bone remodeling in response to

mechanical loading, the explant models have the advantage of isolating the bone (and marrow) from other potential effectors, such as muscle stimulation,^{36,37} the nervous system²⁵ and circulating blood.

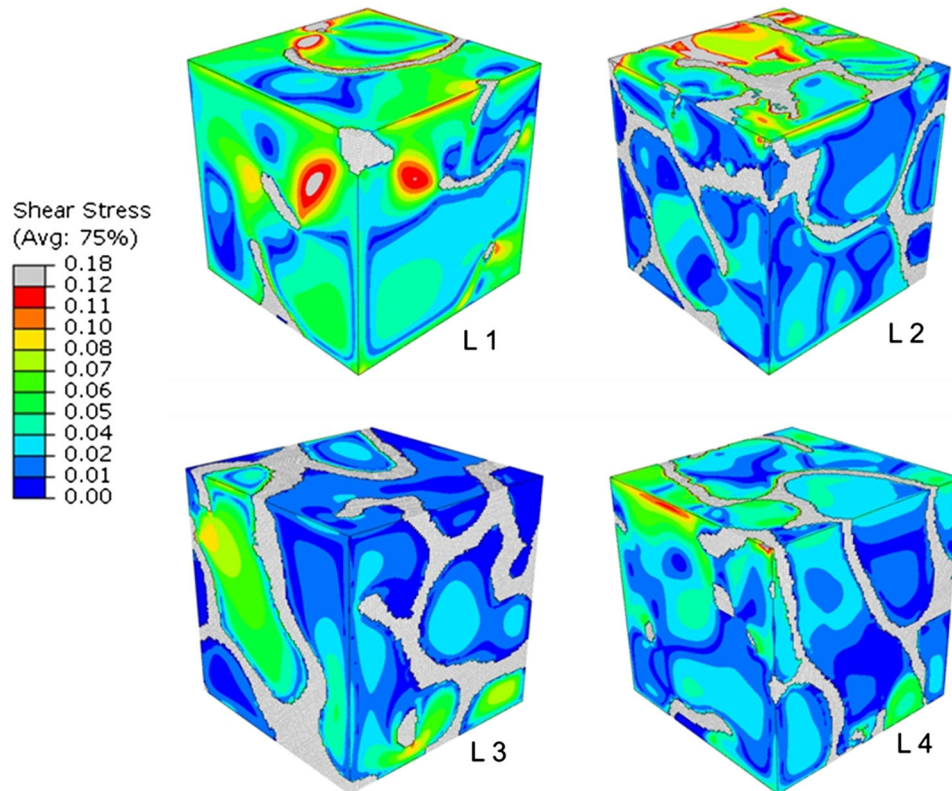
The MAR reported in this study for the samples exposed to a compressive load (approximately 1.0) is of a similar level (0.25–0.94) with previous studies which exposed bone explants to a similar loading regime for a similar duration.^{14,29} The current study has a mean BFR which is higher than reported in these studies by 0.2 $\mu\text{m}/\text{day}$. Additionally, it compares favorably with an *in vivo* study of post-menopausal bone which reported a mean value of 0.53.³⁸

It is of significant interest to compare the experimental data with the computational model predictions. Strains of the magnitude 1000–3000 $\mu\epsilon$ are thought to stimulate new bone formation.^{8,18} However, it should be noted that these studies derived the bone strain at the overall bone scale rather than the micro scale. The strains reported in the current study are derived from a μFE analysis and therefore the use of the 1000–3000 $\mu\epsilon$ range is a major assumption of the current study. Previous studies into trabecular bone formation in response to strain have demonstrated an *in vivo* correlation in a mouse model between bone strain and trabecular bone formation.^{27,28}

Results from the current study demonstrate that 2.2–12.1% of the total bone in the compressively loaded samples was experiencing between 1000 and 3000 $\mu\epsilon$. This increased to 4.3–17.4% when just the bone surface was examined. While no direct correlation was apparent between the average strain magnitudes in a sample and the corresponding bone growth in this study, it was clear that there was sufficient strain generated in certain regions of the bone to stimulate an anabolic response. This suggests that the compressive strain does not have to reach the 1000–3000 $\mu\epsilon$ range throughout the whole trabecular structure to stimulate local bone formation. For example, in the sample (L1) with only 2.2% of the total bone experiencing compressive strain between 1000 and 3000 $\mu\epsilon$, 97.8% of the bone was experiencing compressive strain <1000 $\mu\epsilon$ which is thought to be at a level which leads to resorption however the sample as a whole had a BFR

TABLE 2. The percentage of the bone surfaces experiencing strain within different ranges and the average strain within each sample.

Value of max principal strain ($\mu\epsilon$)		Loaded samples			
		L1	L2	L3	L4
% of bone surface	<1000	93	96	90	83
	1000–3000	7.1	4.3	9.9	17
	>3000	0.09	0.00	0.08	0.05
Average max principal strain ($\mu\epsilon$)		419	462	540	677

**FIGURE 8. Shear stress within the bone marrow of the compressively loaded trabecular bone explants. The bone is colored in white and the marrow mesh is removed for clarity.**

of $0.24 \mu\text{m}/\text{day}$. This indicates that the effects of this strain, which was highest in localized regions, were being transduced throughout the structure. This is likely due to the extensive network of osteocytes throughout the trabecular bone structure.⁴⁰ These cells, ideally placed within the bone,^{6,23,40} are directly stimulated when the bone is under strain⁴³ and are capable of inducing an osteogenic response in MSCs and other marrow resident cells.

2D parallel plate flow chamber experiments which expose cells to shear stress values of 0.1–1 Pa have been shown to stimulate osteogenic responses in MSCs and pre-osteoblastic cells.^{1,2,11} Here, less than 1% of the total marrow, in each compressively loaded

sample, was experiencing shear stress in the stimulatory range of greater than 0.1 Pa. However when the surface alone was examined the percentage experiencing greater than 0.1 Pa increased in all cases, similar to the strain results. Although some portion of the marrow was experiencing stresses greater than 0.1 Pa in all four samples, no significant correlation was apparent between the individual shear stress values in each sample and the corresponding bone growth in this study. However, it was clear that the lower the BV/TV the higher the shear stress experienced by the marrow. This is in agreement with previous studies,^{3,13} although a different trend has been observed elsewhere.³⁰

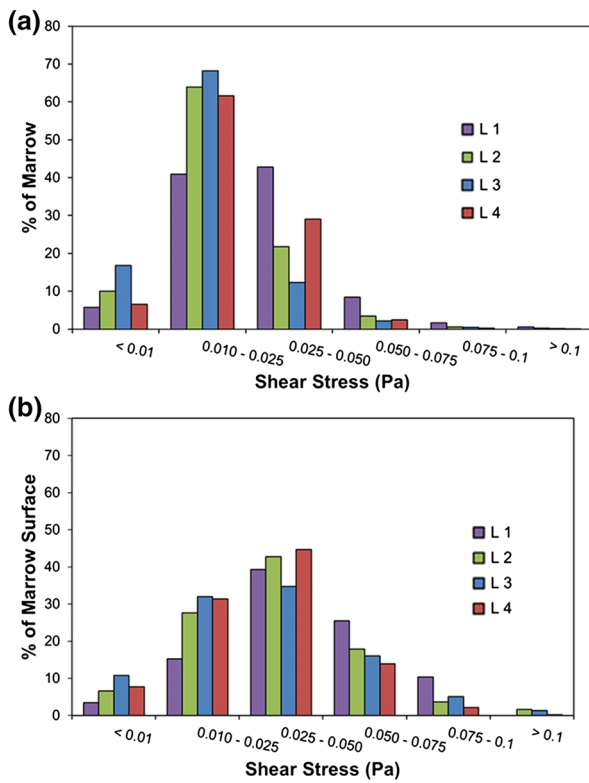


FIGURE 9. Distributions of shear stress within the bone marrow of each compressively loaded trabecular bone ex- plants.

The aim of this study was to assess whether physio- logical compression of trabecular bone generates shear stress within the bone marrow which stimulates new bone growth. It was found within the computa- tional models of the sample specific geometries that shear stress of sufficient magnitude to produce an os- teogenic response in MSCs was indeed generated during physiological compression. However, there was also bone strain of significant magnitude generated during compression which has the potential of being transduced by osteocytes in their extensive network and transmitted through a biochemical response throughout the bone structure. The osteocyte network is well established as capable of detecting, transducing and transmitting a mechanobiological response to MSCs.⁵ It is unknown if localized shear stress effects can be transduced through the marrow. However, re- cent work on the micromechanical modelling of mar- row could provide some insights⁴² into potential networks within the marrow. Given that both marrow shear stress and bone shear strain were present in the current study it was important to assess their relative dominance, and based on the current results it is likely that bone strain is the dominant driver at work to in- duce the anabolic response in bone growth. This is due to the greater amount of bone experiencing strain of sufficient magnitude to generate an anabolic bone

TABLE 3. The percentage of the bone marrow experiencing shear stress within different ranges and the average shear stress within each sample.

Value of shear stress (Pa)		Loaded samples			
		L1	L2	L3	L4
% of marrow	<0.01	5.7	10	17	6.6
	0.01–0.05	84	86	80	91
	0.05–0.10	10	4.0	2.6	2.7
	>0.1	0.58	0.22	0.11	0.04
Average shear stress (Pa)		0.030	0.021	0.018	0.022

TABLE 4. The percentage of the bone marrow surface experiencing shear stress within different ranges and the average shear stress within each sample.

Value of shear stress (Pa)		Loaded samples			
		L1	L2	L3	L4
% of marrow surface	<0.01	3.5	6.6	11	7.8
	0.01–0.05	55	70	67	76
	0.05–0.10	36	21	21	16
	>0.1	6.2	1.6	1.4	0.23
Average shear stress (Pa)		0.050	0.037	0.034	0.032

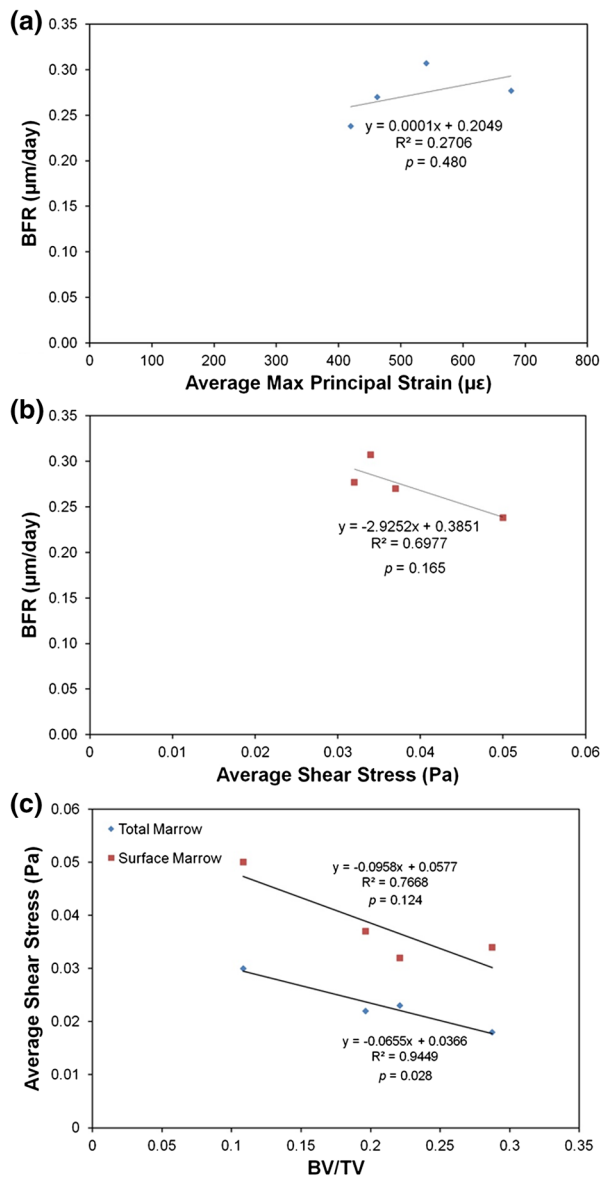


FIGURE 10. (a) No significant correlation was found between surface bone strain and BFR or (b) surface shear stress and BFR. (c) The average shear stress generated at the surface of the marrow and total the total marrow plotted with respect to BV/TV. A significant correlation was found for total marrow shear stress.

growth response, compared to the amount of marrow experiencing shear stress of such a sufficient magnitude.

CONCLUSIONS

In summary *in vivo* responses of trabecular bone to compression loading were simulated in explanted trabecular bone samples as demonstrated by the increase in MAR and BFR. Bone strain and marrow shear stress were highest in the regions at the bone/marrow

surface. The average marrow shear stress was found to decrease for samples with increasing BV/TV, which is consistent with other studies. No significant relationship was apparent between bone growth and individual levels of bone strain or marrow shear stress within each sample, however both bone strain and marrow shear stress were above the minimum stimulatory levels in localized regions for all four loaded samples. On this basis, potential differentiation of MSCs within the marrow may be more likely due to a combination of indirect stimulation (bone strain through the osteocyte network) and direct stimulation (shear stress in the marrow).

Furthermore, given that it was a low percentage of each sample that was shown to experience bone strain and marrow shear stress within the stimulatory range (1000–3000 $\mu\epsilon$ for compressive bone strain and >0.1 Pa for marrow shear stress), it appears that the extensive osteocyte network within the bone structure is in play and is capable of transmitting the local effects of high strain into a biochemical response to stimulate other cells throughout the bone structure. It is not known if such a network exists for the marrow, meaning that the localized regions of high shear stress could indeed remain localized to cells within that area. Further research is required in the area of micromechanical modelling of the multi-cellular bone marrow structure to determine if such a marrow network exists.

ACKNOWLEDGMENTS

The authors would like to acknowledge funding from the Irish Research Council, under the EMBARK program, U.S. National Science Foundation grant CMMI 1100207, Science Foundation Ireland under the Short Term Travel Fellowship and the ORS under the Collaborative Exchange Award.

REFERENCES

- ¹Arnsdorf, E. J., P. Tummala, R. Y. Kwon, and C. R. Jacobs. Mechanically induced osteogenic differentiation—the role of RhoA, ROCKII and cytoskeletal dynamics. *J. Cell Sci.* 122:546–553, 2009.
- ²Bakker, A. D., M. Joldersma, J. Klein-Nulend, and E. H. Burger. Interactive effects of PTH and mechanical stress on nitric oxide and PGE2 production by primary mouse osteoblastic cells. *Am. J. Physiol. Endocrinol. Metab.* 285:E608–E613, 2003.
- ³Birmingham, E., J. A. Grogan, G. L. Niebur, L. M. McNamara, and P. E. McHugh. Computational modelling of the mechanics of trabecular bone and marrow using fluid structure interaction techniques. *Ann. Biomed. Eng.* 41:814–826, 2013.

- ⁴Birmingham, E., T. C. Kreipke, E. B. Dolan, T. R. Coughlin, P. Owens, L. M. McNamara, G. L. Niebur, and P. E. McHugh. Mechanical stimulation of bone marrow in situ induces bone formation in trabecular explants. *Ann. Biomed. Eng.* 2014. doi:10.1007/s10439-014-1135-0.
- ⁵Birmingham, E., G. L. Niebur, P. E. McHugh, G. Shaw, F. P. Barry, and L. M. McNamara. Osteogenic differentiation of mesenchymal stem cells is regulated by osteocyte and osteoblast cells in a simplified bone niche. *Eur. Cell Mater.* 23:13–27, 2012.
- ⁶Bonewald, L. F. Osteocytes as dynamic multifunctional cells. *Ann. N. Y. Acad. Sci.* 1116:281–290, 2007.
- ⁷Bryant, J. D., T. David, P. H. Gaskell, S. King, and G. Lond. Rheology of bovine bone marrow. *Proc. Inst. Mech. Eng. H* 203:71–75, 1989.
- ⁸Burr, D. B., C. Milgrom, D. Fyhrie, M. Forwood, M. Nyska, A. Finestone, S. Hoshaw, E. Saiag, and A. Simkin. In vivo measurement of human tibial strains during vigorous activity. *Bone* 18:405–410, 1996.
- ⁹Carter, D. R., D. P. Fyhrie, and R. T. Whalen. Trabecular bone density and loading history: regulation of connective tissue biology by mechanical energy. *J. Biomech.* 20:785–794, 1987.
- ¹⁰Cartmell, S. H., B. D. Porter, A. J. Garcia, and R. E. Guldberg. Effects of medium perfusion rate on cell-seeded three-dimensional bone constructs in vitro. *Tissue Eng.* 9:1197–1203, 2003.
- ¹¹Case, N., B. Sen, J. A. Thomas, M. Styner, Z. Xie, C. R. Jacobs, and J. Rubin. Steady and oscillatory fluid flows produce a similar osteogenic phenotype. *Calcif. Tissue Int.* 88:189–197, 2011.
- ¹²Chen, J. C., and C. R. Jacobs. Mechanically induced osteogenic lineage commitment of stem cells. *Stem Cell Res. Ther.* 4:107, 2013.
- ¹³Coughlin, T. R., and G. L. Niebur. Fluid shear stress in trabecular bone marrow due to low-magnitude high-frequency vibration. *J. Biomech.* 45:2222–2229, 2012.
- ¹⁴David, V., A. Guignandon, A. Martin, L. Malaval, M.-H. Lafage-Proust, A. Rattner, V. Mann, B. Noble, D. B. Jones, and L. Vico. Ex vivo bone formation in bovine trabecular bone cultured in a dynamic 3D bioreactor is enhanced by compressive mechanical strain. *Tissue Eng. A* 14:117–126, 2008.
- ¹⁵Davies, C. M., D. B. Jones, M. J. Stoddart, K. Koller, E. Smith, C. W. Archer, and R. G. Richards. Mechanically loaded ex vivo bone culture system “Zetos”: systems and culture preparation. *Eur. Cell Mater.* 11:57–75, 2006; (discussion 75, 2006).
- ¹⁶Dickerson, D. A., E. A. Sander, and E. A. Nauman. Modeling the mechanical consequences of vibratory loading in the vertebral body: microscale effects. *Biomech. Model. Mechanobiol.* 7:191–202, 2008.
- ¹⁷Endres, S., M. Kratz, S. Wunsch, and D. B. Jones. Zetos: a culture loading system for trabecular bone. Investigation of different loading signal intensities on bovine bone cylinders. *J. Musculoskelet. Neuronal Interact.* 9:173–183, 2009.
- ¹⁸Fritton, S. P., K. J. McLeod, and C. T. Rubin. Quantifying the strain history of bone: spatial uniformity and self-similarity of low-magnitude strains. *J. Biomech.* 33:317–325, 2000.
- ¹⁹Frost, H. M. Bone, “mass” and the “mechanostat”: a proposal. *Anat. Rec.* 219:1–9, 1987.
- ²⁰Garman, R., G. Gaudette, L.-R. Donahue, C. Rubin, and S. Judex. Low-level accelerations applied in the absence of weight bearing can enhance trabecular bone formation. *J. Orthop. Res.* 25:732–740, 2007.
- ²¹Govey, P. M., A. E. Loisele, and H. J. Donahue. Biophysical regulation of stem cell differentiation. *Curr. Osteoporos. Rep.* 11:83–91, 2013.
- ²²Gurkan, U. A., and O. Akkus. The mechanical environment of bone marrow: a review. *Ann. Biomed. Eng.* 36:1978–1991, 2008.
- ²³Huiskes, R., R. Ruimerman, G. H. van Lenthe, and J. D. Janssen. Effects of mechanical forces on maintenance and adaptation of form in trabecular bone. *Nature* 405:704–706, 2000.
- ²⁴Jones, D. B., E. Broeckmann, T. Pohl, and E. L. Smith. Development of a mechanical testing and loading system for trabecular bone studies for long term culture. *Eur. Cell Mater.* 5:48–59, 2003; (discussion 59–60, 2003).
- ²⁵Kajimura, D., R. Paone, J. J. Mann, and G. Karsenty. Foxo1 regulates Dbh expression and the activity of the sympathetic nervous system in vivo. *Mol. Metab.* 3:770–777, 2014.
- ²⁶Keaveny, T. M., E. F. Morgan, G. L. Niebur, and O. C. Yeh. Biomechanics of trabecular bone. *Annu. Rev. Biomed. Eng.* 3:307–333, 2001.
- ²⁷Lambers, F. M., K. Koch, G. Kuhn, D. Ruffoni, C. Weigt, F. A. Schulte, and R. Müller. Trabecular bone adapts to long-term cyclic loading by increasing stiffness and normalization of dynamic morphometric rates. *Bone*. doi:10.1016/j.bone.2013.04.016.
- ²⁸Lukas, C., D. Ruffoni, F. M. Lambers, F. A. Schulte, G. Kuhn, P. Kollmannsberger, R. Weinkamer, and R. Müller. Mineralization kinetics in murine trabecular bone quantified by time-lapsed in vivo micro-computed tomography. *Bone* 56:55–60, 2013.
- ²⁹Mann, V., C. Huber, G. Kogianni, D. Jones, and B. Noble. The influence of mechanical stimulation on osteocyte apoptosis and bone viability in human trabecular bone. *J. Musculoskelet. Neuronal Interact.* 6:408–417, 2006.
- ³⁰Metzger, T. A., T. C. Kreipke, T. J. Vaughan, L. McNamara, and G. L. Niebur. The in situ mechanics of trabecular bone marrow: the potential for mechanobiological response. *J. Biomech. Eng.* 2014. doi:10.1115/1.4028985.
- ³¹Mohsin, S., F. J. O’Brien, and T. C. Lee. Microcracks in compact bone: a three-dimensional view. *J. Anat.* 209:119–124, 2006.
- ³²Mosley, J. R. Osteoporosis and bone functional adaptation: mechanobiological regulation of bone architecture in growing and adult bone, a review. *J. Rehabil. Res. Dev.* 37:189–199, 2000.
- ³³Nauman, E. A., R. L. Satcher, T. M. Keaveny, B. P. Halloran, and D. D. Bikle. Osteoblasts respond to pulsatile fluid flow with short-term increases in PGE2 but no change in mineralization. *J. Appl. Physiol.* 90:1849–1854, 2001.
- ³⁴Parfitt, A. M., M. K. Drezner, F. H. Glorieux, J. A. Kanis, H. Malluche, P. J. Meunier, S. M. Ott, and R. R. Recker. Bone histomorphometry: standardization of nomenclature, symbols, and units: report of the asbmr histomorphometry nomenclature committee. *J. Bone Miner. Res.* 2:595–610, 1987.
- ³⁵DS SIMULIA. Abaqus 6.12 theory manual. Providence, RI: DS SIMULIA Corp., 2012.
- ³⁶Qin, Y.-X., and H. Lam. Intramedullary pressure and matrix strain induced by oscillatory skeletal muscle stimulation and its potential in adaptation. *J. Biomech.* 42:140–145, 2009.

- ³⁷Qin, Y. X., H. Lam, S. Ferreri, and C. Rubin. Dynamic skeletal muscle stimulation and its potential in bone adaptation. *J. Musculoskelet. Neuronal Interact.* 10:12–24, 2010.
- ³⁸Recker, R. R., D. B. Kimmel, A. M. Parfitt, K. M. Davies, N. Keshawar, and S. Henders. Static and tetracycline-based bone histomorphometric data from 34 normal postmenopausal females. *J. Bone Miner. Res.* 3:133–144, 1988.
- ³⁹Sandino, C., J. A. Planell, and D. Lacroix. A finite element study of mechanical stimuli in scaffolds for bone tissue engineering. *J. Biomech.* 41:1005–1014, 2008.
- ⁴⁰Schaffler, M. B., W.-Y. Cheung, R. Majeska, and O. Kennedy. Osteocytes: master orchestrators of bone. *Calcif. Tissue Int.* 2013. doi:10.1007/s00223-013-9790-y.
- ⁴¹Schulte, F. A., A. Zwahlen, F. M. Lambers, G. Kuhn, D. Ruffoni, D. Betts, D. J. Webster, and R. Müller. Strain-adaptive in silico modeling of bone adaptation—a computer simulation validated by in vivo micro-computed tomography data. *Bone* 52:485–492, 2013.
- ⁴²Vaughan, T. J., M. Voisin, G. L. Niebur, and L. M. McNamara. Multiscale modeling of trabecular bone marrow: understanding the micromechanical environment of mesenchymal stem cells during osteoporosis. *J. Biomech. Eng.* 2015. doi:10.1115/1.4028986.
- ⁴³Verbruggen, S. W., T. J. Vaughan, and L. M. McNamara. Strain amplification in bone mechanobiology: a computational investigation of the in vivo mechanics of osteocytes. *J. R. Soc. Interface* 9:2735–2744, 2012.
- ⁴⁴Vivanco, J., S. Garcia, H. L. Ploeg, G. Alvarez, D. Cullen, and E. L. Smith. Apparent elastic modulus of ex vivo trabecular bovine bone increases with dynamic loading. *Proc. Inst. Mech. Eng. H* 227:904–912, 2013.
- ⁴⁵Webster, D., E. Wasserman, M. Ehrbar, F. Weber, I. Bab, and R. Müller. Mechanical loading of mouse caudal vertebrae increases trabecular and cortical bone mass-dependence on dose and genotype. *Biomech. Model. Mechanobiol.* 9:737–747, 2010.